Published in final edited form as:
Invest Radiol. 2015 January ; 50(1): 40–45. doi:10.1097/RLI.0000000000000093.

Very Low-Dose (0.15 mGy) Chest CT Protocols Using the COPDGene 2 Test Object and a Third-Generation Dual-Source CT Scanner With Corresponding Third-Generation Iterative Reconstruction Software

John D. Newell Jr, MD[*,†], **Matthew K. Fuld, PhD**[‡], **Thomas Allmendinger, PhD**[§], **Jered P. Sieren, BS**[*], **Kung-Sik Chan, PhD**[‖], **Junfeng Guo, PhD**[*], and **Eric A. Hoffman, PhD**[*,†,¶]

[*]Department of Radiology, University of Iowa, Iowa City, IA

[†]Department of Biomedical Engineering, University of Iowa, Iowa City, IA

[‡]Siemens Healthcare, Erlangen

[§]Siemens Healthcare AG, Forchheim, Germany

[‖]Department of Statistics and Actuarial Science, University of Iowa, Iowa City, IA

[¶]Department of Medicine, University of Iowa, Iowa City, IA

Abstract

Objectives—The purpose of this study was to evaluate the impact of ultralow radiation dose single-energy computed tomographic (CT) acquisitions with Sn prefiltration and third-generation iterative reconstruction on density-based quantitative measures of growing interest in phenotyping pulmonary disease.

Materials and Methods—The effects of both decreasing dose and different body habitus on the accuracy of the mean CT attenuation measurements and the level of image noise (SD) were evaluated using the COPDGene 2 test object, containing 8 different materials of interest ranging from air to acrylic and including various density foams. A third-generation dual-source multidetector CT scanner (Siemens SOMATOM FORCE; Siemens Healthcare AG, Erlangen, Germany) running advanced modeled iterative reconstruction (ADMIRE) software (Siemens Healthcare AG) was used.

We used normal and very large body habitus rings at dose levels varying from 1.5 to 0.15 mGy using a spectral-shaped (0.6-mm Sn) tube output of 100 kV(p). Three CT scans were obtained at each dose level using both rings. Regions of interest for each material in the test object scans were automatically extracted. The Hounsfield unit values of each material using weighted filtered back projection (WFBP) at 1.5 mGy was used as the reference value to evaluate shifts in CT attenuation at lower dose levels using either WFBP or ADMIRE. Statistical analysis included basic statistics, Welch *t* tests, multivariable covariant model using the F test to assess the significance of the

Reprints: John D. Newell Jr, MD, Department of Radiology, University of Iowa, 200 Hawkins Dr, CC701GH, Iowa City, IA 52242. john-newell@uiowa.edu.

explanatory (independent) variables on the response (dependent) variable, and CT mean attenuation, in the multivariable covariant model including reconstruction method.

Results—Multivariable regression analysis of the mean CT attenuation values showed a significant difference with decreasing dose between ADMIRE and WFBP. The ADMIRE has reduced noise and more stable CT attenuation compared with WFBP. There was a strong effect on the mean CT attenuation values of the scanned materials for ring size ($P < 0.0001$) and dose level ($P < 0.0001$). The number of voxels in the region of interest for the particular material studied did not demonstrate a significant effect ($P > 0.05$). The SD was lower with ADMIRE compared with WFBP at all dose levels and ring sizes ($P < 0.05$).

Conclusions—The third-generation dual-source CT scanners using third-generation iterative reconstruction methods can acquire accurate quantitative CT images with acceptable image noise at very low-dose levels (0.15 mGy). This opens up new diagnostic and research opportunities in CT phenotyping of the lung for developing new treatments and increased understanding of pulmonary disease.

Keywords

computed tomography; quantitative CT; test object; phantom; lung imaging; emphysema; COPD; radiation dose

---

The new third-generation dual-source computed tomographic (CT) scanners and third-generation iterative reconstruction software enable substantial reductions in radiation dose to the patient.[1] This is of great importance to the medical imaging community because the recent increase in the use of x-ray CT has greatly increased the amount of ionizing radiation received by populations in the United States and other countries around the world.[2,3] The recently published National Lung Cancer Screening Trial study showed a 20% decrease in mortality from lung cancer with the use of screening CT scans of the thorax in patients at high risk for lung cancer.[4–7] The use of CT for lung cancer screening will further increase the number of x-ray CT studies performed on the thorax. Reducing the CT radiation dose to the thorax would be of great benefit to patients enrolled in lung cancer screening programs. Computed tomography is also increasingly being used to establish quantitative phenotypes to subtype lung diseases such as COPD and asthma,[8–15] and reducing the CT dose in these CT studies would also be beneficial.

The medical imaging community has been trying to reduce the amount of ionizing radiation to the general population using a number of approaches. These include using medical imaging studies only when they are known to be beneficial to the patient, substituting nonionizing radiation studies such as ultrasound and magnetic resonance imaging for x-ray CT studies whenever possible, lowering the radiation dose of both radiographic and x-ray CT studies as much as possible while still maintaining adequate image quality and image noise levels, and, finally, encouraging CT manufacturers to pursue advanced technological solutions for reducing the radiation exposures necessary to provide diagnostic images of the thorax and other body parts.

It is very important for quantitative CT scanning of the lung to maintain the accuracy of the CT attenuation values with acceptable levels of image noise. This is accomplished using

carefully designed CT protocols.[16] It is also important to monitor the performance of CT scanners that are used for obtaining quantitative measurements over time. This is typically achieved using CT test objects (CT phantoms) that are made up of nonbiologic materials that simulate different in vivo tissue CT densities such as soft tissue, water, lung tissue, and air. The COPDGene 1 test object in the COPDGene phase 1 multicenter National Institutes of Health study is one of the commonly used CT test objects that is used for CT quality control.[17] This CT test object has been used in a number of National Institutes of Health and privately sponsored multicenter lung research studies that use quantitative CT to phenotype lung disease including COPDGene, multi-ethnic study of atherosclerosis, severe asthma research program, and subpopulations and intermediate outcome measures in COPD study. We have recently described[18] the effects of reducing dose on CT attenuation values in the COPDGene 2 test object using a second-generation dual-source CT scanner, SOMATOM Definition FLASH, and second-generation iterative reconstruction software, SAFIRE.[19] In that study, we showed that the COPDGene 2 test object can be used to assess the effects of decreasing dose on the mean attenuation values of the 8 materials in the COPDGene 2 test object using weighted filtered back projection (WFBP) and using the SAFIRE iterative reconstruction method.

In this study, we have sought to evaluate the quantitative stability of measures derived from the COPDGene 2 test object while lowering imaging to ultralow doses, taking advantage of advances in third-generation dual-source CT technologies including third-generation iterative reconstruction methods.

MATERIALS AND METHODS

Multidetector Computed Tomography Scanner

Scans were performed for 2 days using Siemens SOMATOM FORCE, third-generation dual-source CT scanners located at the Siemens CT manufacturing facility in Forchheim, Germany. The SOMATOM FORCE includes the new Vectron x-ray tubes and Stellar Infinity detectors. The Vectron x-ray tube is a new x-ray tube design that has a very large anode and can accommodate very short exposure times with large anode heat loading. It has high output at 70 kV(p) and 1300 mA, which is 2.9 times the milliampere available at 70 kV(p) for the STRATON tube used on the previous Siemens second-generation dual-source CT scanner, the SOMATOM Definition FLASH. The high milliampere output at the low-kilovolt (peak) setting enables lower doses on large patients compared with the STRATON x-ray tube. The use of an additional 0.6 mm of Sn prefiltration with the new Vectron x-ray tube hardens the x-ray spectrum eliminating lower energy photons that typically are completely absorbed by the patient's body and do not contribute to image formation in noncontrast CT studies of the thorax.[1] The new Stellar Infinity detector incorporates the advantages of integrated circuit design in the original Stellar detector while increasing spatial resolution because of a 25% increase in the number of detector channels and the addition of a 2-dimensional antiscatter grid. In this study, we used the 100-kV(p) spectrum with additional spectral shaping by using 0.6 mm of Sn x-ray beam prefiltration with a mean energy of 79 keV. The Siemens SOMATOM FORCE was only used in the single-energy mode for this study. The dual-energy mode was not evaluated.

Iterative Reconstruction

The 2 main limitations of WFBP are the mathematical non-exactness of the inverse measurement process, which can result in image artifacts (eg, cone beam artefacts), and the handling of the statistical data properties, which are completely ignored.

It is well known from the literature that a theoretical formulation of the problem in the form of a likelihood equation can be derived. This equation describes the relation of image data and measured raw data, taking into account the geometric properties (system model) and its statistical properties (statistical model). The solution of this equation can be derived practically using an iterative approach by means of gradient descent usually referred to as iterative reconstruction. An implementation of this approach by repeated forward and back projection of raw data and image data in combination with statistical modeling and regularization can be found in commercially available statistical iterative reconstruction solutions.[20,21]

The advanced modeled iterative reconstruction (ADMIRE) is built upon these principles, with substantial modifications to enable routine capabilities and improved image quality. The statistical modeling is done in raw data domain, whereas the regularization is extended from the simple localized smoothness constrained toward a more sophisticated localized signal-to-noise analysis on an anatomically relevant length scale. Parameters of the model are set depending on the selected reconstruction algorithm (kernel) that is assigned to clinical applications. The repeated comparison of forward projected pseudoraw data with the measured data for the purpose of removing geometric imperfections (eg, cone beam artifacts) used a special filter with a dedicated weighting in frequency domain, which results in an effective iteration speed that is substantially higher.

The scanner was running a prerelease software version that included standard weighted filtered back projection (WFBP) and the ADMIRE both using a Qr36 reconstruction kernel.

Test Object

The test object (phantom) that was used for this study was the COPDGene 2 test object (Fig. 1). The COPDGene 2 test object is an improved version of the COPDGene 1 test object.[17] The COPDGene 2 test object was manufactured to specifications that were provided to the Phantom Laboratories, Salem, NY. The specifications for improvement of the original COPDGene 1 test object were developed by the COPDGene Imaging Committee and also the National Institute of Standards (NIST) in Gaithersburg, MD. The new features of the COPDGene 2 test object compared with the COPDGene 1 test object include the addition of three 3-cm cylinders of NIST manufactured foams. The 3 NIST foams are referred to as 4-, 12-, and 20-lb foams. These materials are used to generate different CT density references from −937 Hounsfield unit (HU) (4-lb foam), −824 HU (12-lb foam), and −703 HU (20-lb foam), respectively (Fig. 1).

The COPDGene 2 tests object preserves the 12 internal air holes and 6 embedded polycarbonate tubes from the COPDGene 1 test object. The tubes serve in the same capacity as in the COPDGene 1 test object, which is to simulate different airways sizes. Two of the polycarbonate tubes were embedded at a 30-degree angle to the *z* axis of the test object.

Thus, the COPDGene 2 test object contains 8 materials that can be used for a quantitative densitometry study: acrylic (120 HU), water (0 HU), 20-lb foam (−703 HU), 12-lb foam (−824 HU), lung-equivalent foam (−856 HU), 4-lb foam emphysema-equivalent foam (−937 HU), internal air (−1000 HU), and external air (−1000 HU). This range of material densities encompasses the range of densities most assessed with quantitative CT imaging of the lungs. The test object was scanned with 2 different water-equivalent outer ring sizes (average size, 36 cm [ring A]; very large size, 40 cm [ring B]), simulating 2 different body habitus (Fig. 1).

Test Object CT Scan Protocol

The COPDGene 2 test object was secured to the CT table such that the long axis of the test object was parallel to the CT gantry along the *x*-*y* plane of the detector, thus consistent with orientation of routine patient scanning. The table position was adjusted to place the test object in the isocenter of the imaging field of view. The CT scan protocol used a scan collimation of 0.6 mm × 192 slices, 0.75-mm slice thickness with 0.5-mm increment, a pitch of 1.0, 0.5-second rotation time, and 100 kV(p) with tin (Sn) filtration. Without moving the test object with a given outer ring configuration between runs, the object was scanned at 5 different effective milliampere-second values (459, 230, 101, and 47 mAs), corresponding to 4 different x-ray exposures (1.5, 0.75, 0.33, and 0.15 mGy). *Effective milliampere-second* is defined as tube current (milliampere) multiplied by rotation time(s) divided by pitch. Using a 30-cm length to represent an average adult human thorax, the corresponding effective dose range would be 0.63 mSv to 0.06 mSv. For iterative reconstruction, we selected ADMIRE strength of 5 to get the highest amount of noise reduction possible. The data for the study included 3 scans of all 8 materials using each of the outer rings and dose levels, reconstructed with both WFBP and ADMIRE.

Test Object CT Image Segmentation and Analysis

The regions of interest (ROI) used to determine the mean and standard deviation for each material in the test object were extracted using purpose-built segmentation software that made use of threshholding, followed by connected component analysis. The segmented regions were eroded by 4 pixels around the outer edge to eliminate the partial volume effect at the boundary in the *x*-*y* plane. The segmented depth (*z* axis) was 20 mm and was positioned symmetrically around the geometric center of the test object. The number of the voxels in the sampled ROI varied between materials because the size of the lung foam was much larger than the other 7 materials in the test object.

Statistical Methods

A Welch *t* test was used to assess differences between the mean values for a given material, ring size, and dose level when using WFBP or ADMIRE compared with the chosen reference value, which was the 1.5-mGy WFBP image for a given material.

To study the relative effects of ring size, dose level, and material composition on the measured mean values in HU, a multivariable covariance method using the F test to test significance of the following design was used:

$$y_{mean} \sim r_0 + r_1 x_{material} + r_2 x_{ring} + r_3 x_{reconstruction} + r_4 x_{dose}, \text{weights} = \left(r_6 x_{total\_voxels}/sd^2\right) \quad (1)$$

To study the relative effects of ring size, dose level, and material composition on the measured standard deviation of the mean values, the following multivariable covariance method using the F test to test significance was used:

$$\text{Log}(y_{sd}) \sim r_0 + r_1 x_{material} + r_2 x_{ring} + r_3 x_{kvp} + r_4 x_{reconstruction} + s(x, k=3) + \log\left(r_6 x_{total\_voxels}\right) \quad (2)$$

All statistical analyses were conducted in R. A significant statistical difference was assumed if $P < 0.05$.

RESULTS

CT Attenuation Values for Each Material

Table 1 and Table 2 summarize the measured mean attenuation values (mean and SD of 3 repeat scans) of the 8 materials contained in the COPDGene 2 test object using ring A at dose levels of 1.5, 0.75, 0.33, and 0.15 mGy using either ADMIRE (Table 1) or WFBP (Table 2). At 1.5 mGy and 0.75 mGy, there was no significance between the measured attenuation values compared with the predetermined reference value, which was the WFBP CT attenuation value at the highest dose level, 1.5 mGy, for each material except for outside air with WFBP. At the lowest dose level of 0.15 mGy, there were no significant differences between the measured values and the reference values for acrylic, water, and 20-lb foam for both ADMIRE and WFBP. There were significant differences with ADMIRE for 12-lb foam, lung foam, 4-lb foam, inside air, and outside air compared with the corresponding reference value for each material using WFBP at a dose of 1.5 mGy. There were significant differences with WFBP for lung foam, 4-lb foam, inside air, and outside air ($P < 0.05$), compared with the corresponding reference value of each material using WFBP and a dose of 1.5 mGy.

Table 3 and Table 4 summarize the measured mean attenuation values of the 8 materials contained in the COPDGene 2 test object using ring B at dose levels of 1.5, 0.75, 0.33, and 0.15 mGy using either ADMIRE (Table 3) or WFBP (Table 4). At 1.5 mGy, there was no significant difference between the measured attenuation values compared with the predetermined reference value, which was the WFBP CT attenuation value at the highest dose level of 1.5 mGy, for each material except for inside and outside air. At the lowest dose level of 0.15 mGy, there was again no significant difference between the measured values and the reference value for acrylic and water using either ADMIRE or WFBP. There were significant differences with ADMIRE for 20-lb foam, 12-lb foam, lung foam, 4-lb foam, and inside air ($P < 0.05$). There were significant differences with WFBP for 20-lb foam, 12-lb foam, lung foam, 4-lb foam, inside air, and outside air ($P < 0.05$).

Multivariable covariant analysis of the mean CT attenuation values (Tables 1–4) show a significant difference with decreasing dose levels between WFBP and ADMIRE. There was a strong effect on the mean CT attenuation values of the scanned materials for ring size ($P <$

0.0001) and dose level ($P < 0.0001$). The number of voxels in the ROI for the particular material studied did not demonstrate a significant effect ($P > 0.05$).

CT Image Noise (SD)

Image noise (SD within the ROI measurement for each material) increased with a decreasing dose for both WFBP and ADMIRE for all materials studied and for both ring sizes (Figs. 2 and 3). As expected, the noise levels were greater with ring B compared with ring A for all materials using either ADMIRE or WFBP. The ADMIRE had lower noise levels than did WFBP for all materials at all dose levels (Figs. 2 and 3). Multivariable regression analysis of the SD of the ROI for each material at each dose level and for both rings sizes showed a strong effect with different ring size ($P < 0.0001$), dose level ($P < 0.0001$), and reconstruction method ($P < 0.0001$). The number of voxels in the ROI for the particular material studied did not demonstrate a significant effect ($P > 0.05$).

DISCUSSION

Using the COPDGene 2 test object, we have shown in this study that the new third-generation dual-source CT scanner and third-generation iterative reconstruction software enable large reductions in radiation dose while preserving the accuracy of the CT attenuation values compared with WFBP, at comparable dose levels, contained in the COPDGene 2 test object. The new FORCE CT scanner provides acceptable measures of material CT attenuation values at 0.33-mGy exposure. Assuming a 30-cm–length chest dose length product this corresponds to an effective dose of 0.14 mSv, using a chest conversion factor of 0.014. This is equivalent to a standard posterior to anterior and lateral chest radiograph. Using the 0.33-mGy exposure level, the FORCE CT also provides acceptable image noise levels for quantitative metrics of the materials contained in the COPDGene 2 test object. For ring A, representing a chest attenuation equivalent to a patient with a normal body mass index (BMI), quantitative accuracy (1- to 5-HU shift depending on the material) with WFBP is maintained down to an exposure of 0.33 mGy. With ADMIRE, quantitative accuracy (1- to 3-HU shift depending on the material) is maintained down to an exposure of 0.15 mGy, half of the dose from a standard posterior to anterior and lateral chest radiograph. For ring B, representing an x-ray attenuation equivalent to a patient with a very large BMI, quantitative accuracy of 3 to 14 HU, depending on the material, is maintained with WFBP down to an exposure of 0.33 mGy. With ADMIRE, a quantitative accuracy of 0.5 to 11 HU, depending on the material, is maintained down to an exposure of 0.15 mGy. Larger deviations typically occur with lower-density materials (4-lb foam, inside and outside air) and smaller deviations in higher-density materials (acrylic and water).

Our study indicates that the marked reduction in radiation dose is achievable on a third-generation dual-source CT scanner with acceptable image noise, as previously reported for qualitative lung nodule CT studies,[1] while maintaining quantitatively accurate CT lung metrics. This has the potential to greatly reduce the radiation dose to research subjects and patients needing quantitative CT assessment of their lung tissue. Using ring A that is comparable with a subject with a normal BMI, we demonstrate that both WFBP and ADMIRE maintain the accuracy of measures for the full range of material densities down to

a dose of 0.15 mGy. Using ring B that is comparable with subjects with a high BMI, ADMIRE can model more accurately the CT attenuation values of the lower-density materials particularly at the lower doses in large subjects than WFBP can and would be the preferred method between the 2 reconstruction processes for studies of the lung in larger patients when using very low-dose CT protocols on the SOMATOM FORCE CT scanner.

The SOMATOM FORCE with ADMIRE greatly reduces image noise and provides accurate attenuation values for a broad range of materials densities. The technical issues that were addressed in this new generation of dual-source CT scanners to make this possible included solving the inaccuracy of the low-density CT attenuation measurements that were a result of processing and reconstructing the image data using 12-bit data (4096 HU values) resulting in the clipping of HU values below −1024 HU. As we lower the dose, the amount of noise increases and the lower tail of the Gaussian distribution of HU values is clipped in low-density regions, resulting in an upward shift in regional mean density values. The new Stellar Infinity detector, along with a new preprocessing pipeline on the SOMATOM FORCE, solves this issue, in part, by incorporating a 16-bit sinogram reconstruction before interpolating back to the typical 12-bit data (−1024 HU to 3071 HU).

In conclusion, the results of our study indicate that satisfactory quantitative thoracic CT examinations can be performed on third-generation dual-source CT scanners using third-generation iterative reconstruction methods at a dose comparable with that of a 2-view digital projection chest radiograph. There is a significant difference in mean CT attenuation values with ADMIRE compared with WFBP in lower-density materials at lower doses. The ADMIRE values are less shifted than the WFBP values when compared with the reference value used in this study. There are significant decreases in image noise with ADMIRE compared with WFBP at the same dose levels. There is some shift in the mean attenuation values especially for lower-density materials at the lower-dose levels particularly with larger body habitus when WFBPs are used at reduced doses compared with the highest dose studied. This effect is successfully compensated (down to 0.15 mGy) when using ADMIRE. Data from ring A suggest that quantitatively accurate reconstructions in low-density structures can be achieved in populations with normal BMI at all dose levels studied.

Acknowledgments

Supported in part by National Institutes of Health grant R01 HL112986-01A1.

E.A.H. is a founder and shareholder of VIDA Diagnostics, Inc, a company commercializing lung image analysis software developed, in part, at the University of Iowa. J.P.S., K.S.C., and J.D.N. are paid consultants for VIDA Diagnostics, Inc. J.D.N. has stock options with VIDA. J.G. owns VIDA stock. Siemens Healthcare has provided in-kind support for hardware and software residing at the University of Iowa and used in this project.

References

1. Gordic S, Morsbach F, Schmidt B, et al. Ultralow-dose chest computed tomography for pulmonary nodule detection: first performance evaluation of single energy scanning with spectral shaping. Invest Radiol. 2014; 49:465–473. [PubMed: 24598443]
2. Sarma A, Heilbrun ME, Conner KE, et al. Radiation and chest CT scan examinations: what do we know? Chest. 2012; 142:750–760. [PubMed: 22948579]

3. Huda W, Schoepf UJ, Abro JA, et al. Radiation-related cancer risks in a clinical patient population undergoing cardiac CT. AJR Am J Roentgenol. 2011; 196:W159–W165. [PubMed: 21257857]
4. Aberle DR, DeMello S, Berg CD, et al. Results of the two incidence screenings in the National Lung Screening Trial. N Engl J Med. 2013; 369:920–931. [PubMed: 24004119]
5. Church TR, Black WC, Aberle DR, et al. Results of initial low-dose computed tomographic screening for lung cancer. N Engl J Med. 2013; 368:1980–1991. [PubMed: 23697514]
6. Aberle DR, Adams AM, Berg CD, et al. Reduced lung-cancer mortality with low-dose computed tomographic screening. N Engl J Med. 2011; 365:395–409. [PubMed: 21714641]
7. Aberle DR, Berg CD, Black WC, et al. The National Lung Screening Trial: overview and study design. Radiology. 2011; 258:243–253. [PubMed: 21045183]
8. Fan L, Xia Y, Guan Y, et al. Characteristic features of pulmonary function test, CT volume analysis and MR perfusion imaging in COPD patients with different HRCT phenotypes. Clin Respir J. 2014; 8:45–54. [PubMed: 23711228]
9. Hansel NN, Washko GR, Foreman MG, et al. Racial differences in CT phenotypes in COPD. COPD. 2013; 10:20–27. [PubMed: 23413893]
10. Van Tho N, Wada H, Ogawa E, et al. Recent findings in chronic obstructive pulmonary disease by using quantitative computed tomography. Respir Invest. 2012; 50:78–87.
11. Mets OM, de Jong PA, van Ginneken B, et al. Quantitative computed tomography in COPD: possibilities and limitations. Lung. 2012; 190:133–145. [PubMed: 22179694]
12. Martinez CH, Chen YH, Westgate PM, et al. Relationship between quantitative CT metrics and health status and BODE in chronic obstructive pulmonary disease. Thorax. 2012; 67:399–406. [PubMed: 22514236]
13. Rutten EP, Grydeland TB, Pillai SG, et al. Quantitative CT: associations between emphysema, airway wall thickness and body composition in COPD. Pulm Med. 2011; 2011:419328. [PubMed: 21647214]
14. Kim WJ, Hoffman E, Reilly J, et al. Association of COPD candidate genes with computed tomography emphysema and airway phenotypes in severe COPD. Eur Respir J. 2011; 37:39–43. [PubMed: 20525719]
15. Han MK, Kazerooni EA, Lynch DA, et al. Chronic obstructive pulmonary disease exacerbations in the COPDGene study: associated radiologic phenotypes. Radiology. 2011; 261:274–282. [PubMed: 21788524]
16. Newell JD Jr, Sieren J, Hoffman EA. Development of quantitative computed tomography lung protocols. J Thorac Imaging. 2013; 28:266–271. [PubMed: 23934142]
17. Sieren JP, Newell JD, Judy PF, et al. Reference standard and statistical model for intersite and temporal comparisons of CT attenuation in a multicenter quantitative lung study. Med Phys. 2012; 39:5757–5767. [PubMed: 22957640]
18. Sieren JP, Chan KS, Guo J, et al. Influence of radiation dose on mean CT values of lung equivalent foam and other relevant materials contained in the COPDGene 2 test object when reconstructing ct projection data with sinogram affirmed iterative reconstruction (SAFIRE) versus weighted filtered back projection (WFBP). Am J Respir Crit Care Med. 2013; 187:A4876.
19. Sieren JP, Hoffman EA, Fuld MK, et al. Sinogram affirmed iterative reconstruction (SAFIRE) versus weighted filtered back projection (WFBP) effects on quantitative measure in the COPD gene 2 test object. Med Phys. 2014
20. Pickhardt PJ, Lubner MG, Kim DH, et al. Abdominal CT with model-based iterative reconstruction (MBIR): initial results of a prospective trial comparing ultralow-dose with standard-dose imaging. AJR Am J Roentgenol. 2012; 199:1266–1274. [PubMed: 23169718]
21. Thibault JB, Sauer KD, Bouman CA, et al. A three-dimensional statistical approach to improved image quality for multislice helical CT. Med Phys. 2007; 34:4526–4544. [PubMed: 18072519]

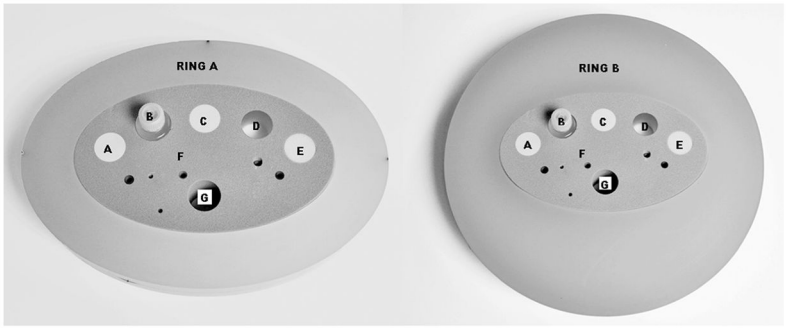

FIGURE 1.

COPDGene 2 test object. Photograph of the COPDGene 2 test object with normal body habitus (ring A) on the left and very large body habitus (ring B) on the right. Each of the 8 materials except for outside air are labeled with capital letters: A indicates 20-lb foam; B, water bottle; C, 12-lb foam; D, acrylic; E, 4-lb foam; F, lung foam; G, inside air.

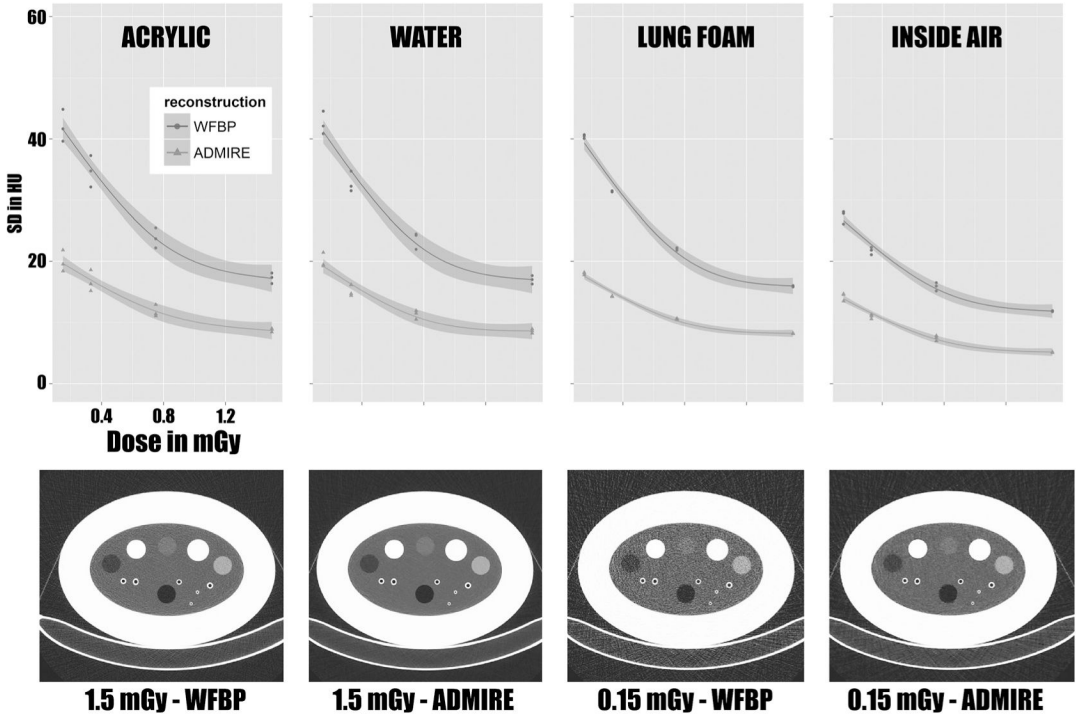

FIGURE 2.

Image noise, ring A. Four top panels are plots of dose versus SD in HU for the corresponding materials acrylic, water, lung foam, and inside air. The top curve with solid red circles represents the WFBP reconstructions and the bottom curve with solid blue triangles represents the ADMIRE reconstructions. The bottom CT images of the COPDGene 2 test object correspond with the 1.5- and 0.15 -mGy reconstructions with WFBP and ADMIRE. Note that the reduction in image noise with ADMIRE is clearly evident in the SD plots and the corresponding CT images.

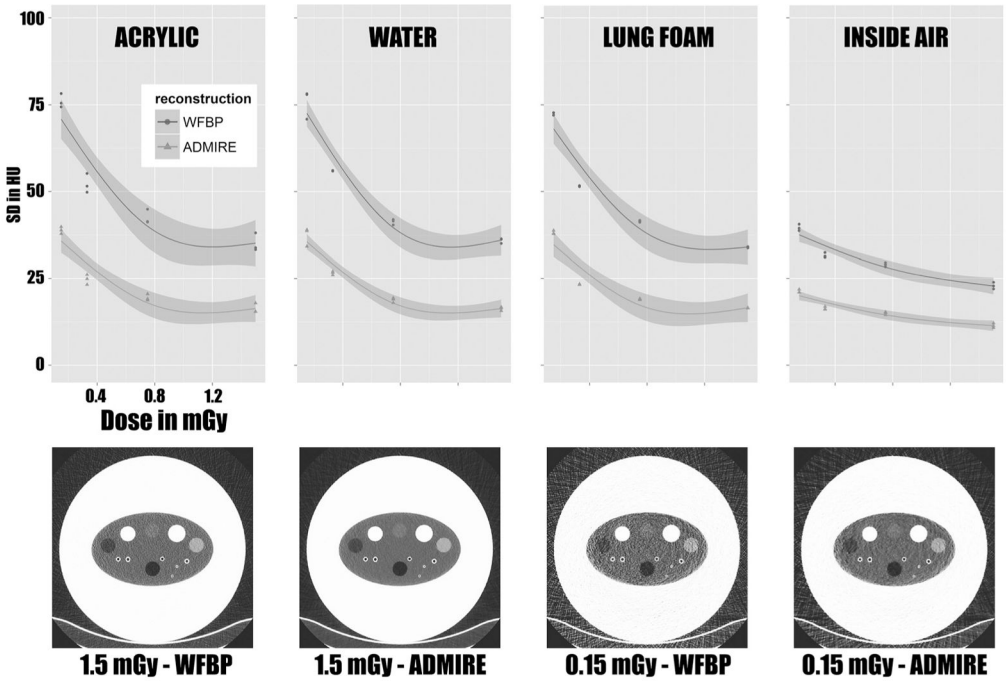

FIGURE 3.

Image noise, ring B. Four top panels are plots of dose versus SD in HU for the corresponding materials acrylic, water, lung foam, and inside air. The top curve with solid red circles represents the WFBP reconstructions and the bottom curve with solid blue triangles represents the ADMIRE reconstructions. The bottom CT images of the COPDGene 2 test object correspond with the 1.5- and 0.15-mGy reconstructions with WFBP and ADMIRE. Note that the reduction in image noise with ADMIRE is clearly evident in the SD plots and the corresponding CT images. As expected, image noise with the very large body habitus ring B is considerably higher than the image noise in Figure 2 that uses the normal body habitus ring A.

TABLE 1

Ring A 100-kV ADMIRE: Median HU and SD of the Different Test Object Materials Scanned Using ADMIRE at Decreasing Dose Levels

Dose Level, mGy	1.5 mGy	0.75 mGy	0.33 mGy	0.15 mGy
Acrylic	125.7 (0.546)	126.8 (0.857)	127.0 (0.924)	125.2 (0.407)
Water	−3.72 (0.504)	−4.03 (1.053)	−3.89 (0.477)	−3.61 (1.295)
20-lb foam	−700.1 (0.595)	−700.7 (0.092)	−700.6 (0.623)	−700.8 (0.217)
12-lb foam	−820.3 (0.250)	−820.6 (0.552)	−820.8 (0.209)*	−821.4 (0.436)*
Lung foam	−853.8 (0.141)	−853.9 (0.165)	−854.3 (0.125)*	−855.8 (0.134)*
4-lb foam	−935.2 (0.223)	−935.3 (0.164)	−935.8 (0.282)*	−938.9 (0.357)*
Inside air	−996.6 (0.353)	−997.1 (0.498)	−997.5 (0.554)*	−997.7 (0.473)*
Outside air	−1000.9 (0.148)*	−1000.2 (0.827)	−1000.1 (0.648)*	−998.4 (1.245)

*$P < 0.05$; Each dose level for each material is compared with the 1.5-mGy (highest) dose level for that material using WFBP.

HU indicates Hounsfield unit; WFBP, weighted filtered back projection.

TABLE 2

Ring A 100-kV WFBP: Median HU and SD of the Different Test Object Materials Scanned Using WFBP at Decreasing Dose Levels

Dose Level, mGy	1.5 mGy	0.75 mGy	0.33 mGy	0.15 mGy
Acrylic	125.5 (0.566)	126.6 (0.874)	126.7 (0.934)	125.0 (0.532)
Water	−3.9 (0.512)	−4.2 (1.068)	−3.9 (0.532)	−3.7 (1.202)
20-lb foam	−699.9 (0.632)	−700.5 (0.141)	−700.1 (0.570)	−700.2 (0.347)
12-lb foam	−820.0 (0.221)	−820.2 (0.584)	−820.2 (0.334)	−820.6 (0.421)
Lung foam	−853.6 (0.145)	−853.7 (0.167)	−854.2 (0.133)*	−855.9 (0.145)*
4-lb foam	−935.1 (0.197)	−935.5 (0.141)	−936.2 (0.301)*	−938.7 (0.512)*
Inside air	−996.1 (0.337)	−995.2 (0.547)	−992.0 (0.648)*	−988.2 (1.029)*
Outside air	−998.6 (0.369)	−996.5 (0.503)*	−994.3 (0.687)*	−989.3 (2.489)*

*$P < 0.05$; Each dose level for each material is compared with the 1.5-mGy (highest) dose level for that material using WFBP.

HU indicates Hounsfield unit; WFBP, weighted filtered back projection.

TABLE 3

Ring B 100-kV ADMIRE: Median HU and SD of the Different Test Object Materials Scanned Using ADMIRE at Decreasing Dose Levels

Dose Level, mGy	1.5 mGy	0.75 mGy	0.33 mGy	0.15 mGy
Acrylic	128.2 (0.404)	127.8 (0.661)	122.9 (0.560)*	132.0 (2.89)
Water	−2.9 (0.420)	−4.4 (0.661)	−8.1 (2.30)	−3.4 (1.11)
20-lb foam	−695.4 (0.375)	−698.2 (0.789)*	−705.8 (0.394)*	−704.9 (1.83)*
12-lb foam	−819.7 (0.225)	−819.1 (0.537)	−823.7 (1.42)*	−829.0 (1.10)*
Lung foam	−848.7 (0.083)	−851.0 (0.106)*	−859.5 (0.192)*	−855.2 (0.479)*
4-lb foam	−930.8 (1.00)	−932.8 (0.806)	−940.8 (1.37)*	−940.3 (2.70)*
Inside air	−995.4 (0.311)*	−995.2 (0.155)*	−999.0 (0.451)*	−995.4 (1.13)*
Outside air	−999.8 (0.507)*	−998.8 (0.701)*	−996.3 (2.47)	−988.7 (2.70)

*$P < 0.05$; Each dose level for each material is compared with the 1.5-mGy (highest) dose level for that material using WFBP.

HU indicates Hounsfield unit; WFBP, weighted filtered back projection.

TABLE 4

Ring B 100-kV WFBP: Median HU and SD of the Different Test Object Materials Scanned Using WFBP at Decreasing Dose Levels

Dose Level, mGy	1.5 mGy	0.75 mGy	0.33 mGy	0.15 mGy
Acrylic	128.1 (0.539)	127.8 (0.685)	123.1 (0.524)*	132.5 (3.15)
Water	−3.0 (0.367)	−4.4 (0.669)	−7.6 (2.53)	−3.0 (0.965)
20-lb foam	−695.0 (0.311)	−698.0 (0.978)*	−705.1 (0.288)*	−704.0 (1.70)*
12-lb foam	−819.0 (0.321)	−818.3 (0.548)	−823.0 (1.48)*	−828.6 (1.01)*
Lung foam	−848.5 (0.83)	−851.0 (0.109)*	−859.6 (0.188)*	−853.9 (0.477)*
4-lb foam	−931.5 (1.05)	−933.0 (0.423)	−939.3 (0.850)*	−932.1 (3.27)
Inside air	−989.8 (0.499)	−985.8 (0.146)*	−986.8 (0.348)*	−980.4 (1.11)*
Outside air	−994.0 (1.92)	−990.4 (1.12)	−980.6 (4.13)*	−965.6 (4.15)*

*P value < 0.05; Each dose level for each material is compared with the 1.5-mGy (highest) dose level for that material using WFBP.

HU indicates Hounsfield unit; WFBP, weighted filtered back projection.